Cellular and Molecular Life Sciences (2023) 80:304
https://doi.org/10.1007/s00018-023-04956-9

ORIGINAL ARTICLE

Selective removal of misfolded SOD1 delays disease onset in a mouse model of amyotrophic lateral sclerosis

Teng Guan[1] · Ting Zhou[1,2] · Xiaosha Zhang[1] · Ying Guo[1,3] · Chaoxian Yang[1,4] · Justin Lin[1] · Jiasi Vicky Zhang[1] · Yongquan Cheng[1] · Hassan Marzban[1] · Yu Tian Wang[5] · Jiming Kong[1,6]

Received: 26 April 2023 / Revised: 26 July 2023 / Accepted: 7 September 2023 / Published online: 26 September 2023

Abstract

Background Amyotrophic lateral sclerosis (ALS) is a devastating neurodegenerative disease. There is no cure currently. The discovery that mutations in the gene *SOD1* are a cause of ALS marks a breakthrough in the search for effective treatments for ALS. SOD1 is an antioxidant that is highly expressed in motor neurons. Human SOD1 is prone to aberrant modifications. Familial ALS-linked SOD1 variants are particularly susceptible to aberrant modifications. Once modified, SOD1 undergoes conformational changes and becomes misfolded. This study aims to determine the effect of selective removal of misfolded SOD1 on the pathogenesis of ALS.

Methods Based on the chaperone-mediated protein degradation pathway, we designed a fusion peptide named CT4 and tested its efficiency in knocking down intracellularly misfolded SOD1 and its efficacy in modifying the pathogenesis of ALS.

Results Expression of the plasmid carrying the CT4 sequence in human HEK cells resulted in robust removal of misfolded SOD1 induced by serum deprivation. Co-transfection of the CT4 and the G93A-hSOD1 plasmids at various ratios demonstrated a dose-dependent knockdown efficiency on G93A-hSOD1, which could be further increased when misfolding of SOD1 was enhanced by serum deprivation. Application of the full-length CT4 peptide to primary cultures of neurons expressing the G93A variant of human SOD1 revealed a time course of the degradation of misfolded SOD1; misfolded SOD1 started to decrease by 2 h after the application of CT4 and disappeared by 7 h. Intravenous administration of the CT4 peptide at 10 mg/kg to the G93A-hSOD1 reduced human SOD1 in spinal cord tissue by 68% in 24 h and 54% in 48 h in presymptomatic ALS mice. Intraperitoneal administration of the CT4 peptide starting from 60 days of age significantly delayed the onset of ALS and prolonged the lifespan of the G93A-hSOD1 mice.

Conclusions The CT4 peptide directs the degradation of misfolded SOD1 in high efficiency and specificity. Selective removal of misfolded SOD1 significantly delays the onset of ALS, demonstrating that misfolded SOD1 is the toxic form of SOD1 that causes motor neuron death. The study proves that selective removal of misfolded SOD1 is a promising treatment for ALS.

Keywords Amyotrophic lateral sclerosis · Misfolded SOD1 · Protein degradation · Chaperone-mediated autophagy · Lysosome

Abbreviations

ALS	Amyotrophic lateral sclerosis
CMA	Chaperone-mediated autophagy

Teng Guan, Ting Zhou and Xiaosha Zhang contributed equally to this work.

✉ Jiming Kong
Jiming.Kong@umanitoba.ca

[1] Department of Human Anatomy and Cell Science, Max Rady College of Medicine, University of Manitoba, Winnipeg, MB, Canada

[2] Department of Pharmacy, The Second Affiliated Hospital of Chongqing Medical University, Chongqing, China

[3] Department of Forensic Medicine, Hebei North University, Zhangjiakou, China

[4] Department of Neurobiology, Southwest Medical University, Luzhou, China

[5] Brain Research Centre and Department of Medicine, Vancouver Coastal Health Research Institute, University of British Columbia, Vancouver, BC, Canada

[6] Department of Human Anatomy and Cell Science, Max Rady College of Medicine, University of Manitoba, 745 Bannatyne Avenue, Winnipeg, MB R3E 0J9, Canada

CTM	Chaperone-mediated autophagy targeting motif
DBR	Derlin-1 binding region
Derlin-1	Degradation in endoplasmic reticulum protein 1
FALS	Familial amyotrophic lateral sclerosis
NSC	Neural stem cell
WT	Wild-type

Introduction

Amyotrophic lateral sclerosis (ALS) is characterized by selective loss of motor neurons leading to muscle weakness, paralysis, and premature death. There is no cure. Mutations in the gene *SOD1* are identified as a cause of familial ALS (FALS) [1]. Strong evidence supports that the FALS-linked SOD1 variants cause the degeneration of motor neurons through a "gain of an adverse property" [2] derived from aberrant conformational changes [3]. The FALS-linked SOD1 variants are readily susceptible to post-translational modifications and become misfolded. Wild-type human SOD1, when oxidatively modified, undergoes conformational changes and acquires the same toxic functions observed for FALS-associated SOD1 variants [4–6]. Misfolded SOD1 is thus considered a toxic factor common to familial and sporadic ALS [4]. This study aims to investigate whether targeted suppression of misfolded SOD1 can serve as a viable approach in the development of successful therapies for ALS.

We have previously reported a novel technique that allows rapid knockdown of endogenous proteins by peptide-directed lysosomal degradation [7]. The technique involves the selective degradation of proteins with KFERQ-like sequences by lysosomes. This is accomplished by fusing a protein-specific peptide to a lysosomal targeting signal, which activates the lysosomal chaperone-mediated autophagy (CMA) pathway and prompts the recognition and degradation of the endogenous protein [8]. The effectiveness of this method is evidenced by the efficient knockdown of both small (α-synuclein, 19kDa) and large (DAPK1, 160kDa) cytoplasmic proteins, as well as the PSD-95, a synaptic scaffolding protein, and the A53T pathological variant of α-synuclein [7].

Recent evidence has revealed that most pathogenic SOD1 mutants share a common feature: their binding to Derlin-1, specifically the CT4 epitope, composed of 12 amino acids (FLYRWLPSRRGG) [9]. The protein–protein interaction (PPI) of misfolded SOD1 is a promising target for drug development as it plays a pivotal role in pathological conditions. This interaction is facilitated by the exposure of a previously concealed Derlin-1-binding region (DBR) located on the N-terminus of SOD1, specifically between amino acids 5 and 18. We designed a fusion peptide (TAT-CT4-CTM, named CT4), which is sensitive to the conformational state of SOD1. CT4 peptide comprises three distinct elements: a cell membrane-penetrating sequence (TAT) that facilitates delivery across the blood–brain barrier and cell membranes, a 12 amino acids Derlin-1-CT4 epitope that selectively targets misfolded SOD1 and a chaperone-mediated autophagy-targeting motif (CTM) that directs the peptide-protein complex towards lysosomal degradation. Here we show that the CT4 peptide directs degradation of misfolded SOD1 in high efficiency and specificity. Administration of the peptide significantly delays disease onset and prolongs the lifespan of the G93A-hSOD1 mouse model of ALS. Our data provide direct evidence that misfolded SOD1 is the toxic form of SOD1 that causes motor neuron death. The study proves that selective removal of misfolded SOD1 is a promising treatment for ALS.

Materials and methods

Animals

All animal experiments followed the "Guide to the Care and Use of Experimental Animals" established by the Canadian Council on Animal Care (CCAC). Transgenic mice carrying the G93A mutation of human SOD1 [B6.Cg-Tg(SOD1*G93A)1Gur/J; 004435] and wild-type human SOD1 (B6.Cg-Tg(SOD1)2Gur/J; 002298) were obtained from Jackson Laboratory. Mouse colonies were maintained in the Central Animal Care Services, University of Manitoba. Mice carrying the human SOD1 transgenes were identified by PCR screening of ear-punched DNA. The mice were monitored with hind limb extension reflex, grip strength, and body weight twice a week from the presymptomatic stage until the end stage. Any initial sign of limb muscle weakness in the grip strength test was considered the onset of ALS disease. Endpoint was defined as when the mouse could not right itself within 30 s when placed on its side, and the bodyweight loss reached 25% of the peak.

Plasmids

HA-CT4-CTM and HA-mCT4-CTM plasmids were constructed by inserting the CT4-CTM or mutant CT4-CTM coding sequence into the pEGFP-N2 vector (Addgene, Watertown, MA) using BglII and EcoRI restriction sites. The CT4-CTM and mCT4-CTM coding sequences were prepared by annealing a custom-designed oligonucleotide duplex (Integrated DNA Technologies, Coralville, Iowa). pEGFP-N2 and CTM-GFP plasmids were prepared as described previously [7]. EGFP-tagged wild-type WT-hSOD1 and G93A-hSOD1 were constructed in the same manner as previously reported [10]. *WT-hSOD1* gene was cloned by RT-PCR from total RNA extracted from

WT-hSOD1 transgenic mouse and subcloned into pEGFP-N1 (Clontech, Palo Alto, CA, USA). Similarly, the *G93A-hSOD1* gene was cloned by RT-PCR from total RNA extracted from G93A-hSOD1 transgenic mice. Plasmids pF141 pAcGFP1 SOD1WT (RRID: Addgene_26402) and pF145 pAcGFP1 G93A-hSOD1 (RRID: Addgene_26406) were a gift from Dr. Elizabeth Fisher. All the plasmid constructions were verified by sequencing. Transfections for transient expression of constructs were performed using FuGENE 6 transfection reagent (Promega, Madison, WI) according to the manufacturer's instructions.

Cell sorting by flow cytometry

GFP positive population of transfected HEK293T cells was sorted by flow cytometry as previously described [11]. Briefly, cultured cells were trypsinized and resuspended in 100µL ice-cold FACS buffer (PBS with 1.5% FBS, 25 mM HEPES pH7.0, and 1 mM EDTA into 75 mm polystyrene round-bottom test tubes. Cells were rinsed twice with 2 mL FACS buffer and resuspended in a final volume of ice-cold 300 µL FACS buffer for analysis. Non-transfected HEK293T cells served as negative controls to calibrate the analyzer for each experiment. The GFP-positive population of cells were sorted based on the expression of GFP. The purity of the sorted populations was analyzed using a BD FACSCanto-II Digital Flow Cytometry Analyzer using FlowJo (Tree Star, USA) software.

Live cell labelling

For lysosomal staining, CHO cells that were transfected with GFP-tagged G93A-hSOD1 were seeded in Nunc Glass Bottom Dishes (Thermo Fisher). After an overnight incubation, the cells were washed three times with PBS. Solutions of the LysoTracker™ Red (Thermo Fisher, #L7528) were prepared from stock solution with prewarmed 10% FBS DMEM. After adding the probe solution, the cells were incubated in a 5% CO_2 atmosphere at 37 °C for 30 min. Then, the supernatant was discarded, and the cells were post-incubated with growth medium in a 5% CO_2 atmosphere at 37 °C for 4 h prior to Live-cell imaging.

Peptide administration

TAT-CT4-CTM (CT4) and TAT-mCT4-CTM (mCT4) peptides were obtained from the Peptide Synthesis and Purification Core Facility at the University of British Columbia. The peptides were administered to the G93A-hSOD1 mice by intravenous (IV) or intraperitoneal (IP) injections. We observed peak body weight in our in-house colony at 100 days of age in young adult presymptomatic mice. Therefore, to test the short-term effect of CT4, 100-day-old G93A mice received IV injections at a dose of 10 mg/kg body weight q.d for three days. To determine the long-term therapeutic effect of CT4 on ALS, the G93A-hSOD1 mice randomly received either mCT4 or CT4 at 10 mg/kg body weight q.o.d through IP injection beginning at 60 days of age until being euthanized at the endpoint. We selected 60 days because we would like to give the presymptomatic animal at least 1 month of treatment before the peak body weight. Gender and litter-balanced mice were assigned to each group.

GST pull-down assay

A nucleotide sequence corresponding to GGGGS-CT4 was cloned in-frame with glutathione S-transferase (GST) in a pGEX-4T-1 vector (Invitrogen, Carlsbad, CA, USA). GST-linked CT4 fusion protein was produced in E. coli, BL21 (DE3, Thermo Fisher) cells by induction with 0.5 mM IPTG at 30 °C at OD600 of about 0.6–0.8 for 6 h. Pellets were then collected by centrifugation and discarding the medium. Pellets were sonicated and centrifuged before purification. For negative control, GST protein was affinity purified simultaneously under similar conditions. GST protein interaction pull-down was done according to the manufacturer's protocols (Thermo Scientific, 21516). The purified protein was monitored with stain-free gel imaging.

Western blot analysis

Mice were deeply anaesthetized with isoflurane and transcardially perfused with ice-cold PBS. Spinal cords and brains were collected and homogenized in 10 volumes of IP lysis buffer (Thermo Fisher, Waltham, MA. Cat# 87787) with 1% (v/v) protease inhibitor cocktails (Thermo Fisher, Waltham, MA. Cat# 78429). Homogenates were centrifuged at 21,000×*g* for 30 min at 4 °C, and supernatants were collected for analysis. For the cell culture samples, cells were washed two times with ice-cold PBS, scraped in lysis buffer, and then transferred into a microcentrifuge tube. The cell suspensions were maintained in agitation for 30 min at 4 °C. Then the cell lysates were centrifuged at 21,000×*g* for 30 min at 4 °C, and the supernatants were collected. After BCA assay (Pierce, Rockford, IL, USA) for protein concentrations, the samples were boiled for 5 min in Laemmli sample buffer containing 2.5% β-mercaptoethanol, separated on 12% TGX Stain-Free polyacrylamide gels (Bio-Rad, Hercules, CA. Cat #1610185), and transferred to PVDF membranes on a Trans-Blot Turbo Transfer System (Bio-Rad). Membranes were blocked with 5% (w/v) fat-free dry milk in Tris-buffered saline (10 mM Tris–HCl, pH 7.5, 150 mM NaCl) containing 0.05% Tween-20 for 1 h and incubated with primary antibodies overnight at 4 °C (see Supplementary Table 1 for the detail of primary antibodies). Blots

were washed thrice in TBST buffer and then incubated with appropriate secondary antibodies for 1 h at room temperature. The protein bands were visualized with the enhanced chemiluminescence reagent (ECL Prime, GE Healthcare. Cat# RPN2232) on an imager (ChemiDoc MP, imaging system, Bio-Rad).

Proximity ligation assay (PLA)

Protein–protein interactions between LAMP2 and misfolded SOD1 were analyzed using Duolink in situ Red Starter Kit (DUO92101, Millipore Sigma Canada Co., Oakville, Ontario). CHO cells were transfected to overexpress G93A-hSOD1 protein tagged with GFP. G93A-hSOD1 overexpressing CHO cells seeded on poly-D-lysine (PDL) coated coverslips were fixed with 4% paraformaldehyde. The cells were washed with PBS and permeabilized using 0.25% Triton X-100 in PBS for 10 min, followed by incubation with Duolink blocking solution in a preheated humidified chamber at 37 °C for 1 h. Primary antibody solution containing mouse-anti-GFP 1:2000 and rabbit-anti-LAMP2 1:200 was added and incubated for 1 h in a preheated humidified chamber at 37 °C. Then, secondary antibodies conjugated with oligonucleotides were added and incubated for 1 h at 37 °C, followed by incubation with a ligation-ligase solution for 30 min at 37 °C, which consists of two oligonucleotides and ligase. In this step, the oligonucleotides hybridize to the two PLA probes and join a closed loop if they are in close proximity. After ligation, the samples were incubated with amplification polymerase solution for 100 min at 37 °C, which consists of nucleotides and fluorescently labelled oligonucleotides. Coverslips were mounted on the slide using Duolink mounting medium with DAPI. The PLA signals were visible as a distinct fluorescent spot, and images were obtained using a Carl Zeiss AxioImager Z2 microscope and processed with Zen Pro imaging software (Zeiss, Germany).

Immunostaining

Cells were fixed in 4% paraformaldehyde in PBS pH 7.4 for 15 min at room temperature and washed thrice with PBS. Samples were incubated for 10 min in PBS containing 0.25% Triton X-100 (PBST) to improve the penetration of the antibody. After three times washing with PBS, coverslips were incubated in 1% BSA in PBST for 30 min to block the unspecific binding of the antibodies. After blocking, samples were incubated with primary antibodies in 1% BSA overnight at 4 as indicated in Supplementary Table 1. Following three additional washes, secondary antibodies were applied and incubated for 1 h at room temperature in the dark. After being washed three final times, cells were incubated with Hoechst 33342 (Thermo Fisher) to counterstain for nuclei, and then coverslips were mounted with a drop of fluorescence mounting medium (Dako North America, Inc. Carpinteria, CA). For spinal cord and sciatic nerves staining, 24 h after the last CT4 injection, lumbar spinal cord and sciatic nerves were isolated, postfixed in 4% PFA for 24 h, dehydrated in 30% sucrose at 4 °C overnight, and embedded in Tissue-Tek (Sakura). Cryosections (14 µm) were thaw-mounted onto coated glass slides (Superfrost Plus, Fisher) and immunohistochemically stained with primary antibodies in 1% BSA overnight at 4 as indicated in Supplementary Table 1. Fluorescence pictures were taken on a Carl Zeiss AxioImager Z2 microscope and processed with Zen Pro imaging software (Zeiss, Germany). Fluorescence intensities were analyzed using the Image J software.

Culture of embryonic neural stem cells

As previously described [12], timed pregnant female C57BL/6 mice mated with G93A-hSOD1 male mice were humanely euthanized by CO_2 gas followed by cervical dislocation, and embryos were removed. The day of the positive vaginal plug was considered as E0.5 of pregnancy, and embryos were collected at E14.5 and placed in Earle's Balanced Salt Solution (EBSS) solution on ice. Transgenic embryos were genotyped by PCR of DNA obtained from tails. The brain was removed, and then cortices were dissected out, triturated, and cells passed through a 40 µM mesh. Cells were maintained in Complete StemPro NSC media containing basic fibroblast growth factor (bFGF) (20 ng/ml) and human epidermal growth factor (hEGF) (20 ng/ml) to maintain NSC characteristics. For differentiation, the NSCs were harvested by centrifugation and plated on a poly-L-ornithine and laminin-coated vessel in the complete StemPro NSC medium. For morphological studies, a total of 150,000 cells were plated on each coverslip, and for biochemical studies, 750,000 cells per 6-well plate well were seeded. The medium was changed to a neural differentiation medium containing 2 mM GlutaMAX-I supplement(GibcoCat# 35050-061) and 2% serum-free B-27 supplement (Gibco Cat # 17504-044) after 2 days of incubation. The cells were fed every third day by aspirating half of the medium from each well and replacing it with a fresh neural differentiation medium. The enriched neuronal culture was confirmed by MAP-2 staining. The spinal cords from E14.5 embryos were dissected and disassociated for myelinating culture [13]. For morphological studies, 150,000 cells were plated on each poly-l-lysine coated coverslip. The cultures were fed thrice weekly by replacing half of the medium.

SOD1 aggregation and thiol oxidation assay

Differential extractions were used to assess SOD1 aggregation as previously described [14, 15]. Cells were scraped

from the culture dish in PBS and centrifuged to pellet the cells before the pellets were resuspended in 100 µl 1 × TEN (10 mM Tris, 1 mM EDTA, and 100 mM NaCl). The resuspended cell culture pellets were then mixed with an equal volume of extraction buffer A (1 × TEN, 1% Nonidet P40, and protease inhibitor cocktail 1:100 dilution) and sonicated with a probe sonicator with 50% output for 30 s (50 W at 20 kHz, FB50, Fisher Scientific, Pittsburgh, PA, USA). The resulting lysate was centrifuged for 5 min at > 100,000 × g in an ultracentrifuge (Optimal L-90k, Beckman Coulter, USA) to separate the pellet (P1) from the supernatant (S1). The supernatant (S1) was decanted and saved for analysis. The pellet (P1) was washed with 200 µl of extraction buffer B (1 × TEN and 0.5% Nonidet P40) by sonication (50% for 30 s). The extract was then centrifuged for 5 min at > 100,000×*g* in a Beckman Airfuge to separate a pellet (P2) from the supernatant. The P2 fraction was resuspended in buffer C (1 × TEN, 0.5% Nonidet P40, 0.25% SDS, and 0.5% deoxycholic acid) by sonication (50% power setting for 30 s) and saved for analysis. Protein concentration was measured in S1 and P2 fractions by the BCA methods as described by the manufacturer (Pierce). For sandwich ELISA, a Human Cu/ZnSOD Matched Antibody Pair Kit (Thermo Fisher, #BMS222MST) was used to detect and quantify protein levels of human Cu/ZnSOD in cell lysates following the manufacturer's protocol. To assess the thiol-disulfide status of the SOD1, aliquots were incubated in an aerobic chamber at room temperature overnight to allow cysteine oxidation. At the same time, anaerobic preserved samples were used as a reference. The capture antibody (SOD1 P222MS, 2.5 µg/mL) was adsorbed on wells of an ELISA plate (F96 cert. MaxiSorp™ Immuno-plate: Nunc, Roskilde, Denmark), to which samples containing the same amount of hSOD1 were applied. Maleimide-activated HRP was then used to determine the thiol content of the captured SOD1 among groups, as the activated HRP presents an available maleimide group that can react with sulfhydryl-containing SOD1. Absorbance was measured on a Synergy Mx multi-mode microplate reader (BioTek).

Histology analysis

Histological examination of the lumbar spinal cord was performed at 149 days of age (median life span, according to our pilot work). For hematoxylin and eosin staining, the tissues (brain, heart, spinal cord, kidney, liver, muscle, lung, and spleen) were fixed overnight in 10% buffered formalin at room temperature and processed for paraffin embedding. Tissues were dehydrated using 70% ethanol for 1 h, 95% ethanol for 3 h, 100% ethanol for 6 h, and xylene for 2.5 h. The tissues were then equilibrated in two melted paraffin baths for 6 h. Tissues were then embedded in paraffin blocks, and paraffin-embedded 5µM sections were stained with hematoxylin solution for 5 min followed by eosin solution for 3 min. The mounted slides were then visualized using light microscopy, and images were taken using a Carl Zeiss M2 microscope and processed with Zen Pro imaging software (Zeiss, Germany). For Nissl staining, the L4 spinal cord segments were collected and fixed in 4% paraformaldehyde (w/v) for 24 h at 4 °C. Samples were cryoprotected in 30% sucrose in PBS solution overnight, embedded in OCT CryoCompound (Sakura CN: 1437355) and cut into 12 µM-thick sections. The sections were stained with a NovaUltra Nissl Stain Kit (IHC WORLD, Woodstock, MD. Cat# IW-3007) and observed on a Carl Zeiss M2 microscope (Zeiss, Germany). Nissl-positive cells were counted in 3 randomly selected sections per sample in the ventral horn of the spinal cord and analyzed using the Image J software.

Statistical analysis

All data collection was performed in a blinded manner. Data are presented as the mean ± SD. For statistical comparison between the two groups, the Student's t-test was used. Multiple comparisons were performed by one-way ANOVA followed by Bonferroni's multiple comparisons test or Two-way ANOVA followed by Sidak's multiple comparisons test. P values less than 0.05 were considered statistically significant for all statistical tests.

Results

A peptide-directed selective knockdown of misfolded SOD1

We designed a peptide-directed chaperone-mediated protein degradation pathway to target misfolded human SOD1 (Fig. 1a). The pathway consists of the transduction domain of HIV TAT protein capable of crossing the cell membrane and the blood–brain barrier [16], the CT4 sequence that selectively binds to misfolded SOD1, and the CMA targeting motif (CTM) destined for lysosomes [7]. The CT4 is a cytosolic carboxyl-terminal region of degradation in endoplasmic reticulum protein 1 (Derlin-1), which is part of a protein complex that mediates endoplasmic-reticulum-associated degradation in chaperone-mediated autophagy [17, 18]. Derlin-1 interacts with virtually all FALS-linked variants of SOD1 [19]. The CT4 epitope of Derlin-1 is composed of 12 amino acids, which is minimally required but sufficient for interaction with misfolded species of human SOD1 derived from either its WT or mutant forms [9]. Human SOD1 contains a masked Derlin-1 binding region (DBR) at amino acids 5–18. When SOD1 becomes misfolded, the conformational DBR epitope is exposed for binding with the CT4

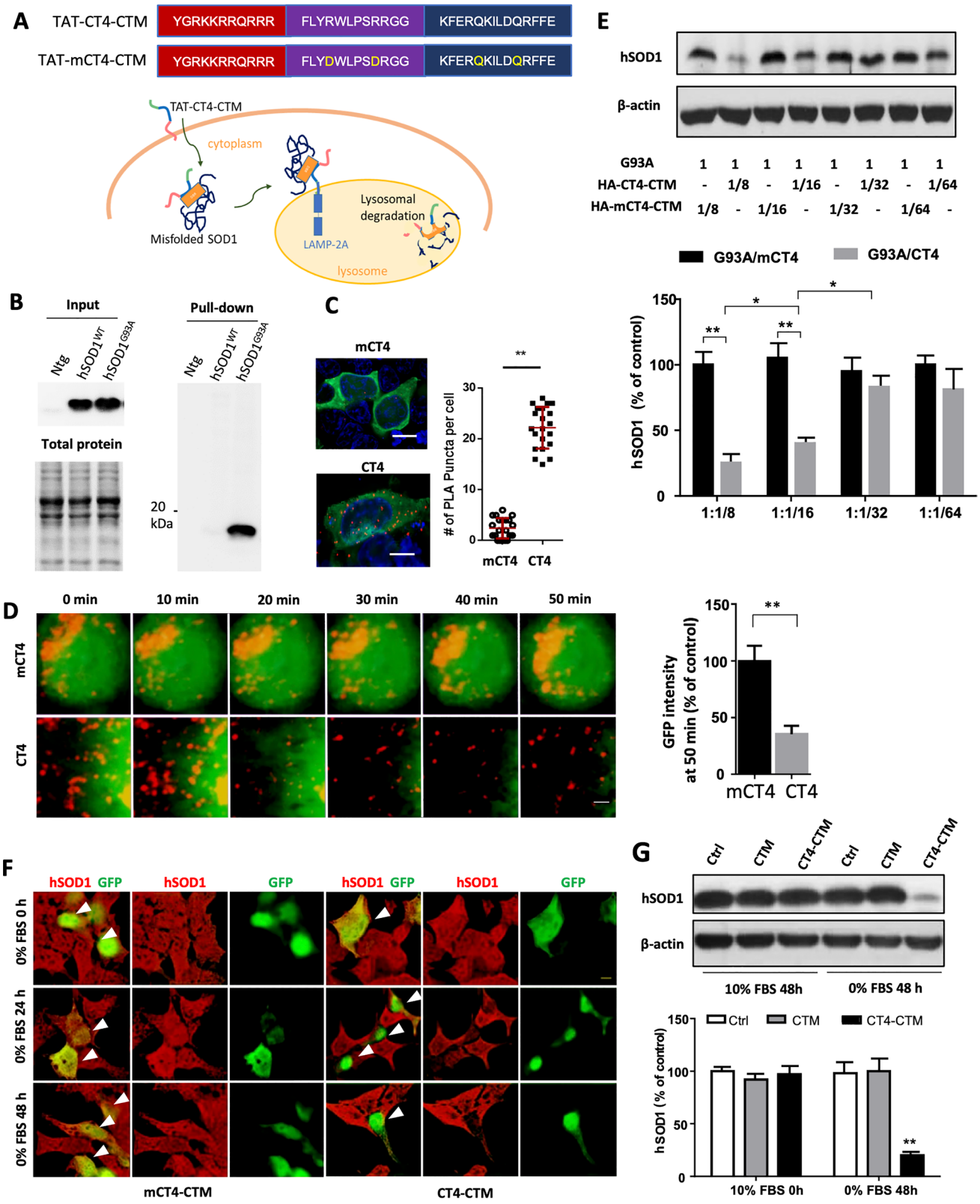
A
TAT-CT4-CTM
YGRKKRRQRRR
FLYRWLPSRRGG
KFERQKILDQRFFE
TAT-mCT4-CTM
YGRKKRRQRRR
FLYDWLPSDRGG
KFERQKILDQRFFE
TAT-CT4-CTM
cytoplasm
Misfolded SOD1
LAMP-2A
Lysosomal degradation
lysosome
B
Input
Pull-down
Ntg
hSOD1WT
hSOD1G93A
Total protein
20 kDa
C
mCT4
CT4
# of PLA Puncta per cell
mCT4 CT4
D
0 min
10 min
20 min
30 min
40 min
50 min
mCT4
CT4
GFP intensity at 50 min (% of control)
mCT4 CT4
E
hSOD1
β-actin
G93A 1 1 1 1 1 1 1 1
HA-CT4-CTM - 1/8 - 1/16 - 1/32 - 1/64
HA-mCT4-CTM 1/8 - 1/16 - 1/32 - 1/64 -
G93A/mCT4
G93A/CT4
hSOD1 (% of control)
1:1/8
1:1/16
1:1/32
1:1/64
F
hSOD1 GFP
hSOD1
GFP
0% FBS 0 h
0% FBS 24 h
0% FBS 48 h
mCT4-CTM
CT4-CTM
G
Ctrl
CTM
CT4-CTM
hSOD1
β-actin
10% FBS 48h
0% FBS 48 h
hSOD1 (% of control)
10% FBS 0h
0% FBS 48h

◂**Fig. 1** CT4-directed CMA system for degradation of misfolded SOD1. **a** Amino acid sequences of the CT4-directed CMA system. The system consists of three motifs: TAT, CT4, and CTM. It is designed to penetrate the plasma membrane, bind with misfolded SOD1, and destinate to lysosome for proteolysis. mCT4, 2Rs were changed into 2Ls within the CT4 epitope as control. **b** Affinity binding assay showed that the GST-tagged CT4 epitope of Derlin-1 pulled down misfolded SOD1 from the G93A-hSOD1 but not the WT-hSOD1 and non-transgenic mice. Input contained total human SOD1 in each spinal cord lysate. Each lane was loaded with 10 µg of protein. n = 4. **c** Co-localization of G93A with LAMP2. CHO cells expressing the GFP-tagged G93A-hSOD1 were treated with 20 µM CT4 peptide or mCT4 for 3 h, followed by proximity ligation assay (PLA) using anti-GFP and anti-LAMP2 primary antibodies. Red spots indicated interactions between GFP and LAMP2. n = 21 cells from 3 experiments. The scale bar represents 5 µm. **d** Live cell imaging on lysosomal degradation of misfolded SOD1. After bath application of CT4 or mCT4 (20 µM) to CHO cells expressing GFP-tagged G93A-hSOD1, the GFP and LysoTracker Red were recorded at intervals of 30 s for 50 min. n = 18 cells from 3 transfections. The scale bar represents 0.2 µm. **e** Levels of hSOD1 in CHO cells 48 h after double transfection with various plasmid ratios of G93A-hSOD1 to HA-CT4-CTM or HA-mCT4-CTM. The membranes were re-probed for β-actin to serve as loading controls. The intensities of the hSOD1 bands were normalized to means of G93A/mCT4 at 1:1/8. n = 9 from 3 independent experiments. Data were analysed with one-way ANOVA followed by Bonferroni's multiple comparison post-test. $^{**}P < 0.001$ $^{*}P < 0.005$. Bars represent mean ± SD. **f** Representative immuno-florescence images of HEK 293T cells transfected with CT4-CTM or mCT4-CTM with serum deprivation for 0 h, 24 h, and 48 h, respectively. Arrows point to positively transfected cells. Scale bar: 10 µm. **g** Levels of hSOD1 in HEK 293T cells 0 h or 48 h after transient transfection with HA-CT4-CTM or HA-CTM. Shown are means ± SD of relative protein levels, normalized to means of the non-transfected; n = 9 from 3 separate cultures. Data were analysed with one-way ANOVA followed by Bonferroni's multiple comparison post-test. $^{**}P < 0.01$. Bars represent mean ± SD

motif of Derlin-1 [20]. For control, we changed 2Rs into 2Ls within the CT4 epitope, hence called mCT4.

We first verified the binding of the CT4 epitope to misfolded SOD1. A GST-linked CT4 (GST-GGGGS-CT4) was immobilized on a glutathione affinity matrix to capture misfolded SOD1. As shown in Fig. 1b, the GST-GGGGS-CT4 pulled down a SOD1 band in protein samples prepared from the spinal cords of the G93A-hSOD1 mice but not from the non-transgenic or the transgenic mice expressing WT-hSOD1. To confirm the CTM signal of the peptide was sufficient for directing the peptide-misfolded SOD1 to lysosomes, CHO cells were transiently transfected with an EGFP-tagged G93A-hSOD1 construct and then treated with CT4 (TAT-CT4-CTM) or mCT4 (TAT-mCT4-CTM) peptide at 20 µM for 3 h. In situ proximity ligation assay (PLA) revealed a robust increase in co-localization of human SOD1 with LAMP2A, the CMA receptor, on lysosomes (Fig. 1c).

We then performed live-cell imaging to label and track the hSOD1 in mCT4 or CT4 peptide-treated cells. The cells were stained with LysoTracker Red to label lysosomes, and the spatial fluorescence patterns of the hSOD1 fusion protein were observed to substantially redistribute and overlap with the LysoTracker Red after CT4 peptide treatment, indicating an increased affinity of hSOD1 for lysosomes. This result was expected, as the CT4 peptide has been shown to enhance the lysosomal targeting of fusion proteins, leading to improved protein degradation and clearance. Quantification of GFP intensity demonstrated a significant decrease by 35.6% at 50 min after the application of CT4, while in the mCT4-treated cells, all images showed diffusely distributed cytosolic G93A-hSOD1. No redistribution nor reduction in expression was observed (Fig. 1d). To determine knockdown efficiency, we co-expressed G93A-hSOD1 with HA-tagged CT4-CTM or mCT4-CTM constructs at different molar ratios in CHO cells. Immunoblot analysis showed that co-expression of CT4-CTM decreased the level of mutant human SOD1 in a dose-dependent manner. Levels of G93A-hSOD1 were reduced by 72.5 ± 3.6% at a 1:1/8 transfection ratio and 56.7 ± 4.4% at a 1:1/16 ratio compared to the cells co-transfected with mCT4-CTM. Levels of mutant SOD1 did not show a significant decrease at ratios of 1:1/32 and 1:1/64 (Fig. 1e).

Serum deprivation is known to induce misfolding of WT-hSOD1[19]. To test the effects of serum deprivation on CT4-directed knocking down of SOD1, we transiently expressed the GFP-tagged CT4-CTM or mCT4-CTM in the human embryonic kidney (HEK) 293T cells, 1 ug total DNA/3×10^5 cells were performed. Twenty-four hours after the transfection, serum deprivation was applied to induce misfolding of endogenous hSOD1. Co-immunofluorescence staining revealed decreased levels of human SOD1 in the CT4-CTM transfected HEK cells (GFP positive) compared to their adjacent non-transfected (GFP negative) cells 24 and 48 h after serum deprivation (Fig. 1f). HEK293T cells transfected with the control plasmid mCT4 did not show a difference compared to non-transfected cells. The result indicates that the CT4-CTM motif could knock down misfolded but not native WT-hSOD1. GFP-positive cells with serum deprivation for 0 h and 48 h were then collected through FACS for Immuno-blot analysis. Results showed that 48 h after serum deprivation, CT4-CTM transfection decreased human SOD1 by 82 ± 2.3% compared to non-transfected cells (Fig. 1g). CTM alone did not induce a reduction of human SOD1. No significant knockdown of human SOD1 was detected in the control group, suggesting no interaction between CT4 and WT-hSOD1.

CT4 peptide potently knocks down misfolded G93A-hSOD1 endogenously expressed in neurons

We determined the knockdown efficacy of CT4 on human SOD1 endogenously expressed in neurons. Neurons were prepared from mouse embryonic neuron stem cells (NSC) expressing the G93A mutation of human SOD1. Application of the CT4 peptide to the neurons for 3 h revealed a

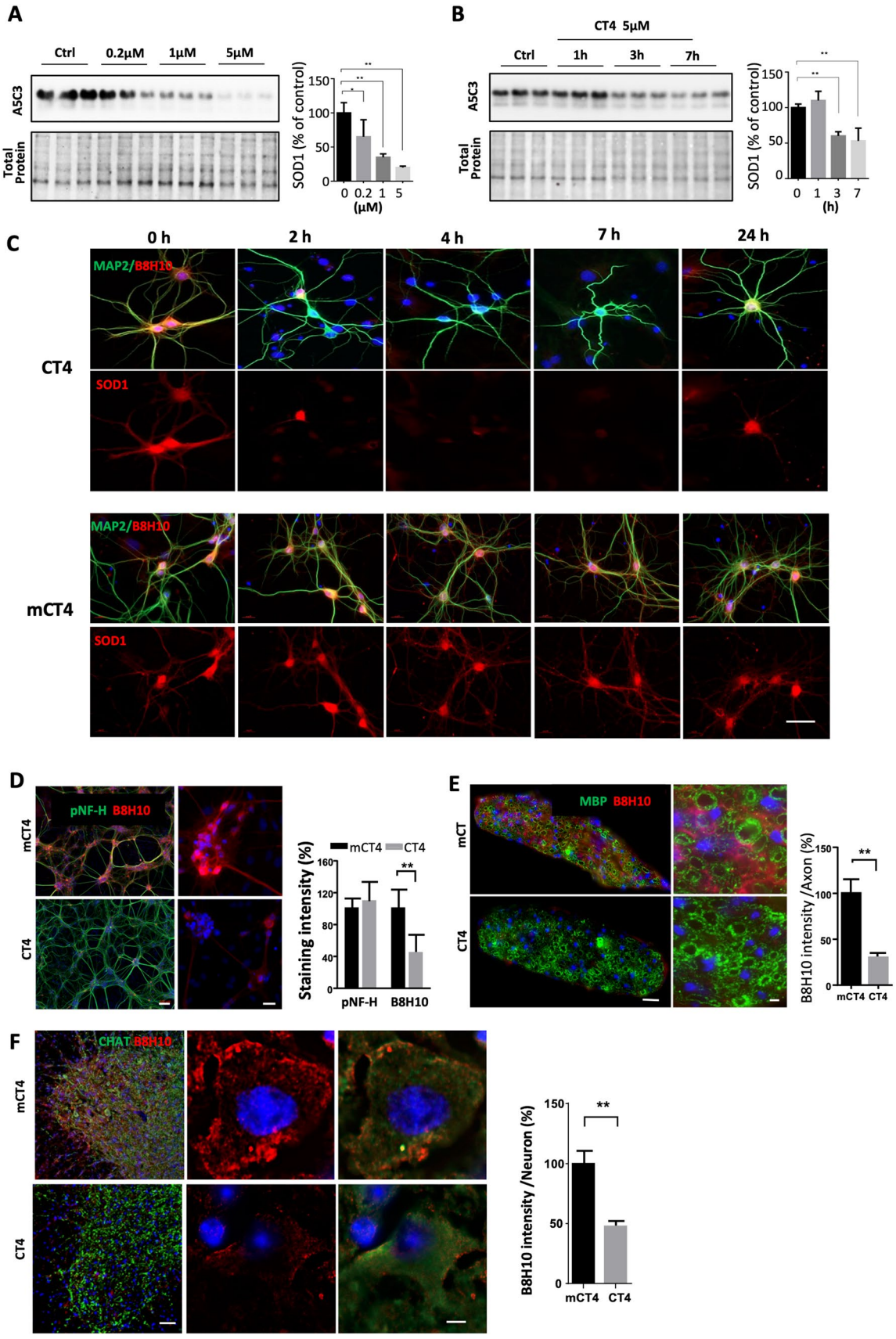
A
Ctrl
0.2μM
1μM
5μM
A5C3
Total Protein
SOD1 (% of control)
(μM)
B
CT4 5μM
Ctrl
1h
3h
7h
(h)
C
0 h
2 h
4 h
7 h
24 h
MAP2/B8H10
SOD1
CT4
mCT4
D
pNF-H B8H10
mCT4
CT4
Staining intensity (%)
pNF-H
B8H10
E
MBP B8H10
mCT
CT4
B8H10 intensity /Axon (%)
F
CHAT B8H10
mCT4
CT4
B8H10 intensity /Neuron (%)

◂**Fig. 2** CT4 removes misfolded SOD1 endogenously expressed in neurons. **a** Dose-dependent knockdown on SOD1 endogenously expressed in neurons. Neurons prepared from transgenic mice expressing G93A-hSOD1 were treated with CT4 at 0 μM, 0.2 μM, 1 μM, or 5 μM for 3 h. **b** Time-course of CT4-directed knockdown of misfolded SOD1 in primary neurons expressing G93A-hSOD1. n = 9 cultures prepared from 3 mice. Blots in **a**, **b** were probed with the A5C3 antibody. Data were analyzed with one-way ANOVA followed by Bonferroni's multiple comparison post-test. *P < 0.05; **P < 0.01. n = 9 cultures prepared from 3 mice. **c** Levels of misfolded SOD1 in neurons expressing G93A-hSOD1 after treatment with CT4 (5 μM). The neurons were immunostained with B8H10 (red) and MAP2 (green) antibodies. Scale bar = 20 μm. **d** Immunofluorescence staining with antibodies to pNF-H (green) and misfolded SOD1 (B8H10, red) after treatment with CT4 in myelinating culture. Scale bar = 100 μm (for lower magnification) and 20 μm (for higher magnification). **e**, **f** Knockdown of misfolded SOD1 in the sciatic nerve and spinal cord of the G93A-hSOD1 mice treated by intravenous injection of CT4 or mCT4 at 10 mg/kg body weight daily for three days at the age of 100 days. **e** Sciatic nerves were harvested at 24 h afterwards. Sections of sciatic nerves were immunostained with antibodies to MBP (green), and misfolded SOD1 (red) was detected with the B8H10 antibody. Shown are staining intensities of misfolded SOD1 in axons. n = 4 mice. Scale bars equal 20 μm (for lower magnification) and 5 μm (for higher magnification). **f** Spinal cord sections were immunolabeled with an antibody to CHAT (Green), and misfolded SOD1 (red) was detected with the B8H10 antibody. Shown are staining intensities of misfolded SOD1 in CHAT-positive neurons. n = 4 mice. Scale bar: 100 μm (lower magnification) and 10 μm (higher magnification). Data in **d**–**f** represented mean ± SD and was analyzed with a two-tailed Student's t-test. **p < 0.01

dose-dependent decrease of SOD1. Exposure to CT4 peptide, even at a low concentration (0.2 μM) for 3 h, reduced G93A-hSOD1 by 31%. At 5 μM, the knockdown efficacy increased to over 79% (Fig. 2a). Time-course analysis of primary neurons exposed to CT4 at 5 μM showed that levels of SOD1 decreased significantly 3 h after exposure to CT4 (Fig. 2b). Consistent with the western blot analysis, immunofluorescence staining with antibodies to MAP2 and to misfolded SOD1 (B8H10, MediMabs) revealed that the expression of G93A-hSOD1 was reduced throughout neurons in the presence of the CT4 peptide. Cells were treated with CT4 peptide for 2 h at 5 μM and then analyzed at different recovery time points (Fig. 2c). We selected a treatment duration of 2 h based on pilot studies conducted in our laboratory, which indicated that this period was necessary for achieving the desired effect. Noticeably, expression of G93A-hSOD1 recovered 24 h after initial exposure to CT4. Cells that acquired MAP2-positive immunoreactivity in the control group had no changes in the expression of misfolded SOD1 as detected by the B8H10 fluorescence intensity (Fig. 2c). Treatment of CT4 dose- and time-dependently reduced misfolded SOD1, and the peptide treatment did not appear to show toxicity to the cells. Differentiating neural stem cells (NSC) to neurons, astrocytes, and oligodendrocyte lineages, further analysis showed that exposure to CT4 peptide resulted in significant reduction of misfolded SOD1 in astrocytes but not in oligodendrocyte precursor cells and mature oligodendrocytes (Supplementary Fig. 1A). We further tested the effect of CT4 on levels of SOD1 in a myelinating culture prepared from the G93A-hSOD1 mice spinal cord. As expected, exposure to CT4 at a final concentration of 5 μM resulted in a significant reduction of misfolded SOD1 (Fig. 2d). We verified the cell type-specific knockdown in the G93A-hSOD1 mice that received CT4 intravenously for 3 days at 10 mg/kg body weight. Spinal cord samples were collected at 24 h after the last injection. Immunostaining confirmed the reduction of misfolded SOD1 in spinal cord motor neurons (Fig. 2f) and astrocytes (Supplementary Fig. 1B), as well as in sciatic nerve (Fig. 2e).

CT4 preferentially reduces detergent-soluble species of misfolded SOD1 through lysosomes

To determine the aggregation propensity of misfolded SOD1, CHO cells were transiently transfected with wild-type human SOD1 and G93A constructs. Non-transfected cells were used as controls. Both WT-hSOD1 and the G93A-hSOD1 variant were present in the soluble fraction (S1) as detected with an antibody (Abcam AB52950) recognizing human SOD1. In the insoluble fraction (P2) fraction, however, hSOD1 was only detected 48 h post-transfection in the G93A-expressing cells (Fig. 3a). To verify this result, we used a pan-SOD1 antibody (ThermoFisher MA1-105), which recognizes both human SOD1 and hamster SOD1. As expected, in the soluble fraction (S1), hSOD1 was detected in WT-hSOD1 and G93A-hSOD1 transfected groups. At the same time, hamster SOD1 was present in all groups (Fig. 3b). Noticeably, in the insoluble fraction (P2), hSOD1 was only detected 48 and 72 h after transfection in the cells expressing G93A-hSOD1. In addition, a SOD1 band in the insoluble fraction (P2) was detected at a position corresponding to the SOD1 dimer, indicating that dimerization and aggregation of the misfolded G93A-hSOD1 could take up to 48 h (Fig. 3b). These data reveal that misfolded SOD1 has a higher aggregation propensity compared with native human SOD1.

We further tested the role of lysosomes in the CT4-directed degradation of misfolded SOD1. Neuron-enriched cultures prepared from embryonic neural stem cells of the G93A-hSOD1 mice were treated with ammonium chloride (NH_4Cl), a lysosomotropic inhibitor, at 10 mM and then exposed to CT4 at 5 μM for 3 h. As shown in Fig. 3c, treatment with the CT4 peptide alone significantly reduced the levels of SOD1, especially in the soluble fractions. Pre-treatment of cells with NH_4Cl blocked the knockdown efficacy of CT4 on misfolded SOD1. Nutrient deprivation by incubating the cells in Earle's Balanced Salt Solution (EBSS) to activate lysosomal activity led to significantly decreased SOD1 levels in all fractions (Fig. 3c).

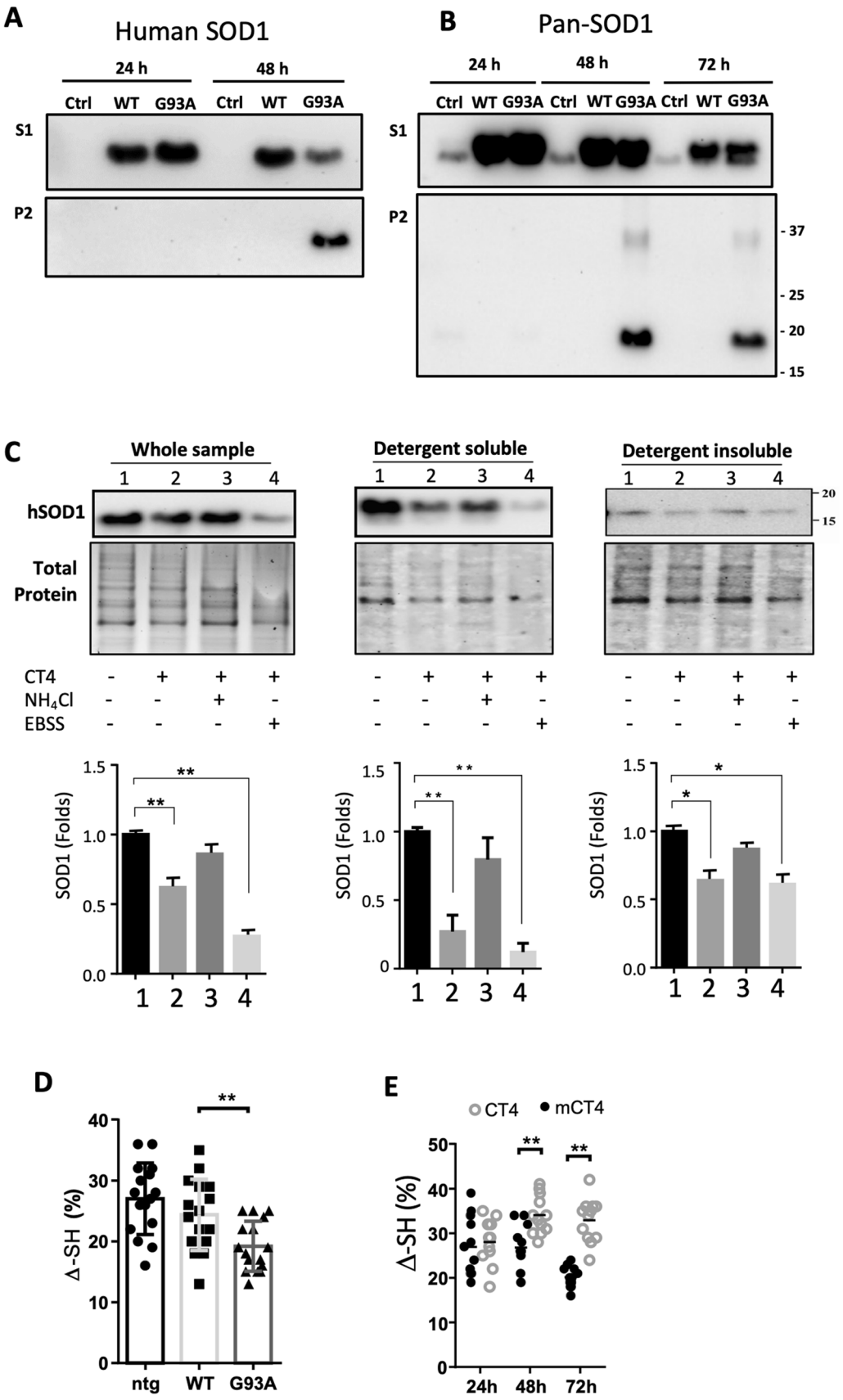
A
Human SOD1
24 h
48 h
Ctrl WT G93A Ctrl WT G93A
S1
P2
B
Pan-SOD1
24 h
48 h
72 h
Ctrl WT G93A Ctrl WT G93A Ctrl WT G93A
S1
P2
37
25
20
15
C
Whole sample
Detergent soluble
Detergent insoluble
1 2 3 4
hSOD1
Total Protein
20
15
CT4 - + + + - + + + - + + +
NH4Cl - - + - - - + - - - + -
EBSS - - - + - - - + - - - +
SOD1 (Folds)
1.5
1.0
0.5
0.0
**
**
**
**
*
*
1 2 3 4
D
Δ-SH (%)
40
30
20
10
0
**
ntg
WT
G93A
E
CT4
mCT4
Δ-SH (%)
50
40
30
20
10
0
**
**
24h
48h
72h

◂**Fig. 3** CT4 removes misfolded SOD1 in detergent-soluble fraction through lysosomes. **a**, **b** ALS-linked G93A-hSOD1 is detectable in both detergent-insoluble (P2) and soluble (S1) fractions. CHO cells were transfected with constructs of WT-hSOD1 and G93A-hSOD1 for indicated hours. Blots were probed with the antibody that recognizes only hSOD1 (**a**) or pan-SOD1 antibody recognizing both human and hamster SOD1 (**b**). **c** Neurons differentiated from embryonic NSCs of the G93A-hSOD1 mice were pretreated with or without 10 mM NH_4Cl or EBSS for 1 h, followed by treatment with 5 μM CT4 for 3 h. After treatment, total cellular extracts, detergent-soluble and insoluble fractions from cells were prepared. Equal volumes of lysates with a total of 10 μg protein were loaded to 12% TGX stain-free polyacrylamide gels. Total protein generated by stain-free visualization was used as loading controls. Data on SOD1 expression were analyzed with one-way ANOVA followed by Bonferroni's multiple comparison post-test. $^{**}P < 0.01$. Bars represent mean ± SD. n = 3. **d** A modified immunosorbent assay was used to detect the thiol-disulfide status of the SOD1 in non-transgenic, WT-hSOD1, and G93A-hSOD1 cell lysates. The thiol content was normalized to total hSOD1, measured using a commercial ELISA kit. One-way ANOVA followed by Bonferroni's multiple comparison post-test was performed to establish significant differences with the non-transgenic (ntg) group: $^{*}P < 0.05$. Bars represent mean ± SD, n = 6 from 3 separate cultures. **e** The aerobic/anaerobic ratio was measured by incubating neuron lysate in an aerobic chamber overnight, and anaerobic preserved aliquots were used as references. Two-way ANOVA followed by Sidak's multiple comparisons test was performed. $^{**}P < 0.01$. n = 6 from 3 separate cultures

Our previous study showed that oxidative modification of cysteine 111 promoted the formation of disulfide bond-independent aggregation of SOD1 [21]. We assessed the effects of CT4 peptide on the thiol-disulfide status of SOD1. The G93A variant of human SOD1 showed a significant reduction in the aerobic/anaerobic ratio of thiols (Δ-SH) compared to the WT-hSOD1 in thiol oxidation assay (Fig. 3d). Bath-application of CT4 to the G93A-hSOD1 neurons at 5 μM for 48 or 72 h markedly increased the aerobic/anaerobic ratio of thiols when compared with the mCT4 control (Fig. 3d), suggesting a selective removal of oxidized SOD1 by CT4.

CT4 robustly reduces misfolded SOD1 and delays disease onset, and prolongs lifespan in the G93A-hSOD1 mouse model of ALS

We first tested the knockdown efficacy of CT4 administered intraperitoneally on misfolded SOD1. At 100 days of age, G93A-hSOD1 mice received either mCT4 or CT4 at 10 mg/kg body weight daily for three days. Tissues were harvested at 24 h, 48 h, 1 week, and 2 weeks after the last injection. For the brain, frontal and temporal cortices were analyzed, and for the spinal cord, lumbar sections were collected for the experiment. Levels of misfolded SOD1, as detected by western blot with an antibody specific for misfolded SOD1 (A5C3, MediMabs) in the spinal cord, brain, liver, and muscle of the G93A-hSOD1 transgenic mice, had significantly reduced levels of SOD1 at 24 h and 48 h after CT4 treatment compared with groups treated with mCT4 (Fig. 4). The A5C3 antibody reacted specifically against misfolded SOD1 when loading amount of protein was below 10 μg (Supplementary Fig. 2). Levels of misfolded SOD1 recovered 1 week or 2 weeks (data not shown) after CT4 peptide treatment (Fig. 4).

We then tested the effects of CT4 on disease onset and progression in the G93A-hSOD1 mouse model of ALS. Mice received IP injections of CT4 or mCT4 at 10 mg/kg q.o.d from 60 days of age until the endpoint. Any initial sign of limb muscle weakness was considered the onset of ALS disease. As shown in Fig. 5a, mice treated with CT4 significantly delayed reaching the peak body weight and the onset of disease. As reflected by the duration from 10% body weight loss to the endpoint, disease progression was also slowed down ($p < 0.05$). Notably, chronic treatment with CT4 significantly extended the lifespan of the G93A-hSOD1 mice by an average of 22.5 days compared to those treated with mCT4 (n = 13 for mCT4 group and n = 15 for CT4 group; $P < 0.01$). No gender difference in survival was seen in G93A mice. Histological examination of the lumbar spinal cord of mice at 149 days of age (median life span, according to our pilot work) showed that there were significantly more ventral horn neurons in the CT4-treated than in the mCT4-treated animals. However, there was a significant loss of ventral horn neurons in the CT4-treated mice compared with that in the WT-hSOD1 mice (Fig. 5b). Consistent with the changes in ventral horn neurons in the lumbar spinal cord, there was a 70% increase (an increase of 93 axons, $P < 0.01$) in the L5 ventral root in the CT4-treated group compared with mCT4 control (Fig. 5c). There were no signs of toxicity observed in cells and in all the animals receiving either CT4 or mCT4. Wild-type mice treated with CT4 or mCT4 at the same concentration daily for 113 days did not show any pathological changes in the brain, heart, spinal cord, kidney, liver, muscle, lung, and spleen (Supplementary Fig. 3).

Discussion

In the present study, we have designed a peptide-directed chaperone-mediated protein degradation pathway for intracellularly misfolded human SOD1. We have provided in vitro and in vivo evidence demonstrating its efficacy in selectively knocking down misfolded SOD1. Importantly, administration of the CT4 peptide significantly delays disease onset in the G93A-hSOD1 mouse model of ALS. To our knowledge, this is the first study that targets selectively misfolded SOD1. Our data provide direct evidence that misfolded SOD1 is the toxic form of SOD1 that causes motor neuron death.

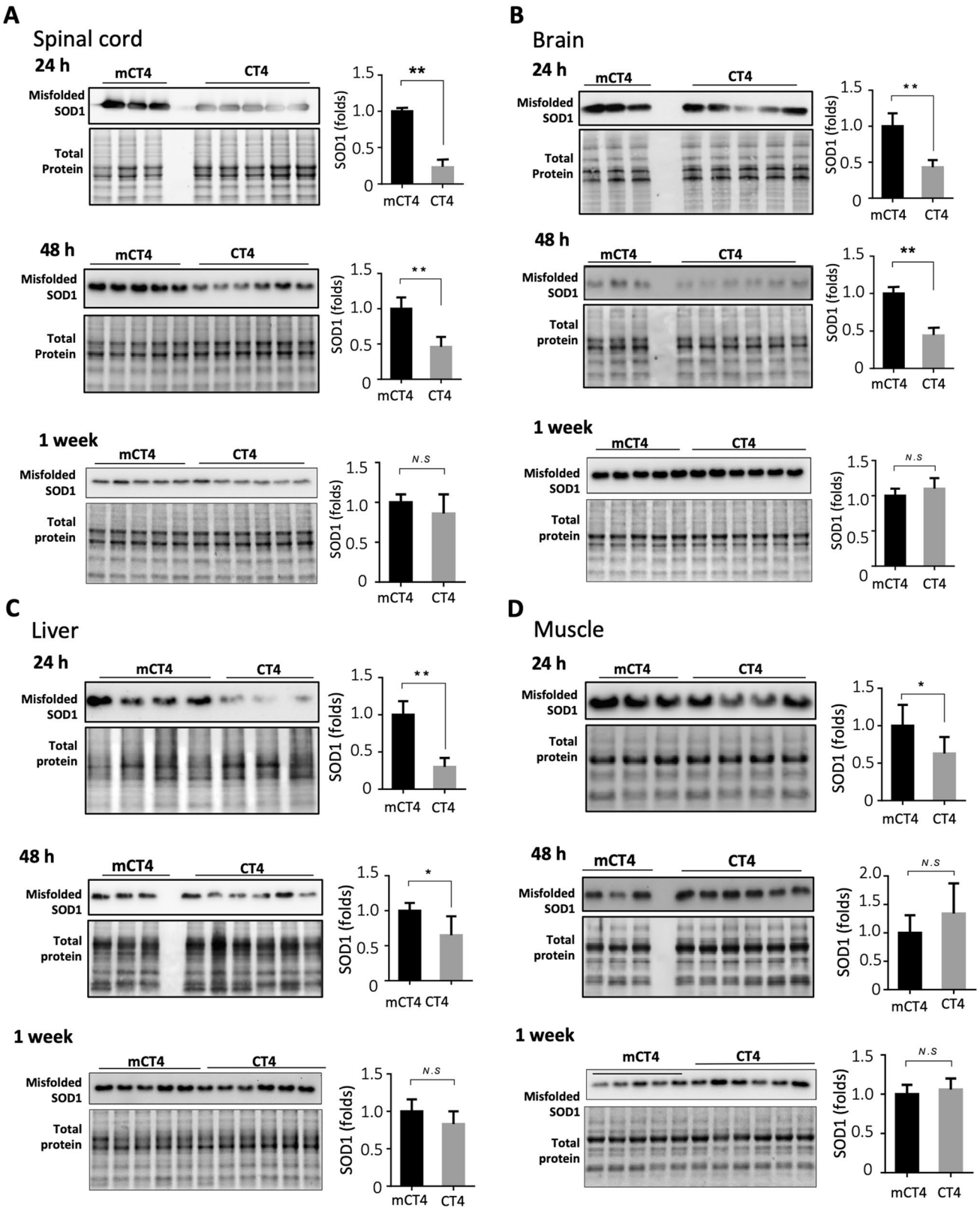

Because mutations in the gene *SOD1* are a cause of familial ALS (FALS) [1], targeting SOD1 is a rational strategy towards effective treatments for patients with ALS. Removal of SOD1, achieved by targeting the *SOD1* gene [22, 23] or mRNA [24–30], has effectively slowed the disease progression and extended survival in animal models of ALS and

◂**Fig. 4** CT4 reduces misfolded SOD1 in the G93A-hSOD1 mouse model of ALS. The G93A-hSOD1 mice received intravenous injections of either mCT4 or CT4 at a dose of 10 mg/kg body weight daily for three days at the age of 100 days. Spinal cord (**a**), brain (**b**), liver (**c**), and muscle (**d**) tissues were harvested at 24 h, 48 h and 1 week afterwards. Misfolded SOD1 was detected by western blot analysis using an antibody specific for misfolded SOD1 (A5C3, MediMabs). Equal volumes of lysates with a total of 10 µg protein were applied to 12% TGX Stain-Free polyacrylamide gels. Total protein by stain-free visualization was used for loading controls. A two-tailed t-test was performed to establish significant differences with the control group: *P < 0.05; **P < 0.01. Bars represent mean ± SD, n = 5–8 animals per group

produced evidence of clinical improvement. By delivering an adeno-associated virus vector encoding RfxCas13d programmed to target superoxide dismutase 1 (SOD1) to the mouse spinal cord, the researchers observed more than 50% reduction in SOD1 mRNA and protein levels, which improved outcomes in the ALS mouse model [31]. These strategies, however, are not designed to target selectively the pathogenic species of SOD1. Meanwhile, ablation of the *SOD1* gene may compromise the anti-oxidation system and accelerate ageing [32]. At the protein level, immunization protocols aiming to reduce the burden of extracellular SOD1 variants [33, 34] or misfolded SOD1 [35] have been shown to alleviate disease symptoms and prolong lifespans in animal models of ALS. However, the potential to develop this immunological strategy into a cure for ALS is limited since it does not target misfolded SOD1 intracellularly. Targeted clearance of misfolded SOD1 could be an effective treatment for ALS. Maier et al. screened for human memory B cells in a significant number of healthy elderly individuals and developed a recombinant human monoclonal antibody (α-miSOD1) that selectively targeted misfolded SOD1 and not physiological SOD1 dimers. After administering the antibody to animal models of ALS, the researchers observed that it postponed the start of motor impairments, extended the animals' survival, and reduced the degeneration of neurons and the accumulation of SOD1 aggregates [36]. Although the researchers' analysis was limited to postmortem spinal cord samples and the detection of misfolded SOD1, they observed that administering the mouse α-miSOD1 antibody directly into the brain ventricles of G93A-hSOD1 mice delayed muscle atrophy and improved motor impairments. However, it's worth noting that the delivery of α-miSOD1 was through osmotic minipumps starting at 60 days of age. Despite this treatment, the median survival of the mice only increased by 7 days compared to the control littermates that received the vehicle treatment. Our approach targets specifically the pathogenic species of SOD1 and can be administered systematically through peptide-based therapeutics. By utilizing the cellular machinery, CT4 peptide promotes the degradation of misfolded SOD1 without disrupting normal cellular processes, which reduces the risk of cell damage and toxicity. The 37 amino acids CT4 peptide can be generated using various techniques, including peptide synthesis and purification from bacterial expression systems. The efficacy and safety of TAT-mediated transduction of therapeutic peptides have recently been elucidated in a successful human clinical trial [37], making the CT4 peptide a clinically promising therapy for ALS.

Although the nature of the gain-of-function toxicity in mutant SOD1 variants is not fully understood, increasing evidence suggests that aberrant posttranslational modifications of SOD1 are a critical step towards gaining such a toxic property. Our studies and others show that ALS-linked mutant SOD1 proteins are readily susceptible to posttranslational modifications [10, 21, 38, 39]. One such modification is the oxidation at its cysteine residues [10]. Human SOD1 has four cysteine residues, Cys6, Cys57, Cys111, and Cys146. An internal disulfide bond exists between Cys57 and Cys146, which contributes to the high stability of the SOD1 protein. This disulfide bond is highly conserved in SOD1 from various organisms, while the other two cysteines are free and not conserved. Cysteine contains a thiol group (Cys-SH) that can be reversibly oxidized to a sulfenic acid (Cys-SOH) by low concentrations of hydrogen peroxide or irreversibly to sulfinic (Cys-SO_2H)/sulfonic (Cys-SO_3H) acids by high concentrations of hydrogen peroxide [40–42]. SOD1 can be oxidized by its own reaction product, hydrogen peroxide [43, 44]. Our studies found that the G93A and the G37R mutations of human SOD1 are more susceptible to oxidative modification than WT-hSOD1. Oxidized G93A-hSOD1 is readily detectable in transgenic mice at the age of 8 weeks, which correlates well with the formation of SOD1 aggregates in spinal cord motor neurons at this stage [45]. We found that cysteine 111 is particularly susceptible to oxidation [21], which provokes misfolding and aggregation of the SOD1 proteins[46, 47]. The late-onset and age-dependent penetrance of the disease argues that the ALS-linked SOD1 mutants are not initially toxic until post-translationally modified. In addition to oxidative modification, aberrant conformations of SOD1 can also be induced by demetallation [48, 49] and other altered post-translational modifications under conditions such as starvation and ischemia [20, 39]. Studies further show that the misfolded SOD1 could be derived from either mutant SOD1 or the wild-type human SOD1 [5, 50]. WT-hSOD1, when modified post-translationally, undergoes aberrant conformational changes and acquires the same toxic functions that are observed for FALS-associated SOD1 variants [4, 5, 48]. The misfolded "mutant-like" WT-hSOD1 has been detected in human postmortem tissues from sporadic ALS individuals [4, 51], suggesting that such species are pathogenic. Because ageing is the most significant risk factor in the pathogenesis of ALS and oxidative stress is currently considered the

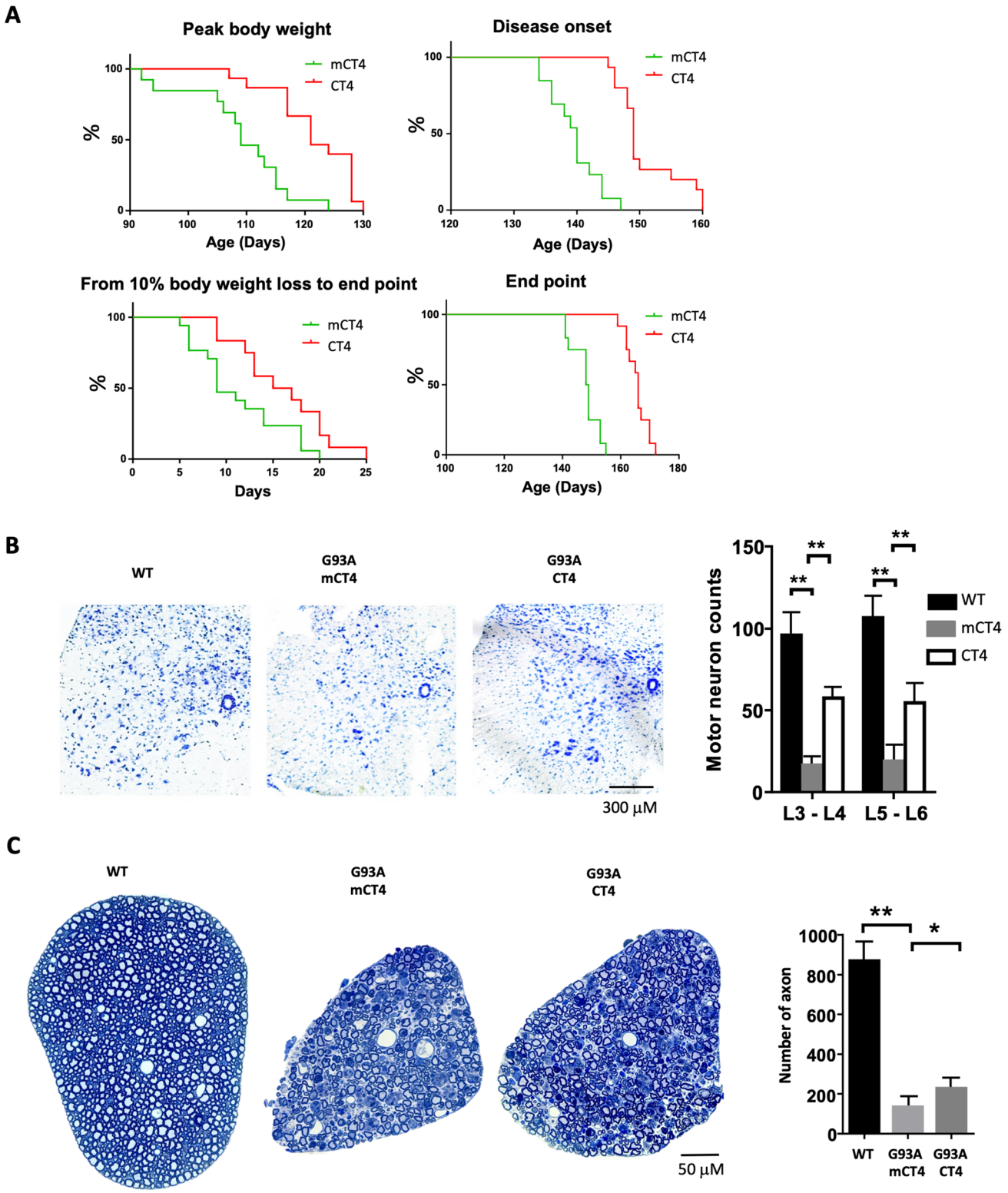

most prominent theory of ageing, post-translational oxidation of SOD1 seems a plausible causing factor in familial and sporadic ALS [6, 38, 52]. Therefore, the knockdown of misfolded SOD1 would be a therapeutic strategy for both familial and sporadic forms of ALS.

Specificity is the most crucial property of the targeting peptide system. The degree to which targeting peptides can successfully reduce targeted pathogenic SOD1 proteins is predominantly influenced by the strength and precision of the bond between the misfolded SOD1 binding domain and

◂**Fig. 5** CT4 significantly delays disease onset and prolongs lifespan in the G93A-hSOD1 mouse model of ALS mice. Beginning at 60 days of age, the G93A-hSOD1 mice received intraperitoneal injections of either mCT4 or CT4 peptide (10 mg/kg) q.o.d until endpoint. **a** Kaplan–Meier plots of ages with peak body weight, disease onset ages, and days between 10% body weight loss to endpoint and endpoint ages. n = 13 for the mCT4 group and n = 15 for CT4 group. Log-rank (mantel-Cox) test was performed: $P < 0.01$ for peak weight, $P < 0.01$ for the onset, $P < 0.05$ for the 10% body weight loss to the endpoint, and $P < 0.01$ for the endpoint. **b** CT4 significantly increases the number of neurons in the ventral horn of the L3–4 and L5–6 spinal cord in 149-day-old G93A-hSOD1 mice treated with mCT4 or CT4. Shown are the numbers of Nissl-stained cells in the ventral horn per section. Two-way ANOVA followed by Sidak's multiple comparisons test was performed. N = 4 mice in each group. $^{**}P < 0.01$. **d** Axonal degeneration in L5 ventral roots at different stages of ALS in mCT4 or CT4 treated G93A-hSOD1 mice at 149 days of age. Plastic sections were stained with toluidine blue, and all myelinated axons were counted. A two-tailed t-test was performed to assess the significant differences between mCT4 and CT4 peptide-treated groups. N = 4 mice in each group. $^{*}P < 0.05$; $^{**}P < 0.01$

the intended proteins. The derlin-1 CT4 epitope can interact with 124 SOD1 mutants out of all 132 studied [19]. Amongst the CT4-interactive mutants, the most common ALS-related forms, such as A4V, G93A, G37R, and G85R, are included. The eight SOD1 mutants identified not to interact with CT4 were only identified in individual patients [19]. Unlike the G93A mutant, the eight non-CT4-interactive SOD1 mutants did not induce endoplasmic reticulum stress or death of motor neurons in E12.5 mouse spinal cord cultures [19], suggesting those mutant forms are not as toxic as the common mutant G93A. Thus, the mutant SOD1 targets of CT4 include necessary toxic forms. In our study, CT4-CTM overexpression was able to knock down misfolded WT-hSOD1 induced by serum deprivation but not the native WT-hSOD1. This supports a previous finding that CT4 binds to the exposed DBR of misfolded SOD1 induced by serum deprivation. The utilization of Derlin-1 CT4 epitope as a "capture" motif in the present study provides a high specificity to ALS-related misfolded SOD1.

The accumulation of detergent-insoluble SOD1 aggregates is a common feature of ALS that may act as a transmissible agent between neurons [53]. As such, both the detergent-soluble and -insoluble SOD1 may be potentially toxic and are considered one of the mechanisms by which mutant/misfolded SOD1 causes ALS [15]. Using aggregation assay, we demonstrated that mutant SOD1 was prone to form the detergent-insoluble aggregates 48 h after transfection with G93A-hSOD1 plasmid. Our data revealed that CT4 peptide could reduce both soluble and insoluble SOD1 levels, although the knockdown is more efficient for soluble SOD1.

In this study, we administered CT4 peptide prior to the onset of motor deficits, and the treatment successfully delayed the onset of the disease. Notably, in the majority of the CT4 peptide-treated animals, muscle weakness occurred after 10% body weight loss, while mCT4-treated controls showed the opposite trend. Although the CT4 treatment significantly delayed the onset of the disease, it only marginally extended the disease progression. This partial efficacy may be due to several reasons, including a decline in lysosomal activity during the late disease stage, which could limit the therapeutic effect of CT4 peptide. Additionally, the stability of peptides has been a challenge, but recent advancements in various modification techniques have made it possible to increase their stability. Therefore, it is important to focus on enhancing the therapeutic potential of CT4 peptide by further exploring these techniques.

Conclusions

The CT4 peptide directs the degradation of misfolded SOD1 with high efficiency and specificity. Selective removal of misfolded SOD1 significantly delays the onset of ALS, demonstrating that misfolded SOD1 is the toxic form of SOD1 that causes motor neuron death. The study proves that selective removal of misfolded SOD1 is a promising treatment for ALS.

Supplementary Information The online version contains supplementary material available at https://doi.org/10.1007/s00018-023-04956-9.

Acknowledgements The authors would like to acknowledge the assistance of Dr Lynda Kong in editing the manuscript.

Author contributions TG coordinated the project and drafted the manuscript. TZ performed most of the in vivo experiments. XZ conducted plasmid construction and in vitro validation. YG, CY, YC aided in animal experiments. JL, JVZ helped cell-based experiments. HM, YTW made a conceptual contribution and reviewed the manuscript. JK initiated and supervised the project. All authors read and approved the final manuscript.

Funding The study was supported by Grants from ALS Society of Canada, Brain Canada and By-Health China.

Availability of supporting data All data published in the paper will be available upon request.

Declarations

Conflict of interest The authors declare no competing interests.

Ethical approval and consent to participate All our work was reviewed and approved by the animal use subcommittee at the University of Manitoba.

Consent for publication The authors consent to publishing this work.

References

1. Gurney ME, Pu H, Chiu AY, Dal-Canto MC, Polchow CY, Alexander DD, Caliendo J, Hentati A, Kwon YW, Deng HX (1994) Motor neuron degeneration in mice that express a human Cu, Zn superoxide dismutase mutation. Science 264(5166):1772–1775

2. Wong PC, Pardo CA, Borchelt DR, Lee MK, Copeland NG, Jenkins NA, Sisodia SS, Cleveland DW, Price DL (1995) An adverse property of a familial ALS-linked SOD1 mutation causes motor neuron disease characterized by vacuolar degeneration of mitochondria. Neuron 14(6):1105–1116
3. Julien J-P (2001) Amyotrophic lateral sclerosis: unfold the toxicity of the misfolded. Cell 104:581–591
4. Bosco DA, Morfini G, Karabacak NM, Song Y, Gros-Louis F, Pasinelli P, Goolsby H, Fontaine BA, Lemay N, McKenna-Yasek D et al (2010) Wild-type and mutant SOD1 share an aberrant conformation and a common pathogenic pathway in ALS. Nat Neurosci 13(11):1396–1403
5. Guareschi S, Cova E, Cereda C, Ceroni M, Donetti E, Bosco DA, Trotti D, Pasinelli P (2012) An over-oxidized form of superoxide dismutase found in sporadic amyotrophic lateral sclerosis with bulbar onset shares a toxic mechanism with mutant SOD1. Proc Natl Acad Sci USA 109(13):5074–5079
6. Ezzi SA, Urushitani M, Julien JP (2007) Wild-type superoxide dismutase acquires binding and toxic properties of ALS-linked mutant forms through oxidation. J Neurochem 102(1):170–178
7. Fan X, Jin WY, Lu J, Wang J, Wang YT (2014) Rapid and reversible knockdown of endogenous proteins by peptide-directed lysosomal degradation. Nat Neurosci 17(3):471–480
8. Dice JF, Terlecky SR, Chiang HL, Olson TS, Isenman LD, Short-Russell SR, Freundlieb S, Terlecky LJ (1990) A selective pathway for degradation of cytosolic proteins by lysosomes. Semin Cell Biol 1(6):449–455
9. Nishitoh H, Kadowaki H, Nagai A, Maruyama T, Yokota T, Fukutomi H, Noguchi T, Matsuzawa A, Takeda K, Ichijo H (2008) ALS-linked mutant SOD1 induces ER stress- and ASK1-dependent motor neuron death by targeting Derlin-1. Genes Dev 22(11):1451–1464
10. Chen X, Zhang X, Li C, Guan T, Shang H, Cui L, Li XM, Kong J (2013) S-nitrosylated protein disulfide isomerase contributes to mutant SOD1 aggregates in amyotrophic lateral sclerosis. J Neurochem 124(1):45–58
11. Basu S, Campbell HM, Dittel BN, Ray A (2010) Purification of specific cell population by fluorescence activated cell sorting (FACS). J Vis Exp. 10(41):1546
12. Li W, Guan T, Zhang X, Wang Z, Wang M, Zhong W, Feng H, Xing M, Kong J (2015) The effect of layer-by-layer assembly coating on the proliferation and differentiation of neural stem cells. ACS Appl Mater Interfaces 7(5):3018–3029
13. Thomson CE, McCulloch M, Sorenson A, Barnett SC, Seed BV, Griffiths IR, McLaughlin M (2008) Myelinated, synapsing cultures of murine spinal cord—validation as an in vitro model of the central nervous system. Eur J Neurosci 28(8):1518–1535
14. Karch CM, Borchelt DR (2008) A limited role for disulfide cross-linking in the aggregation of mutant SOD1 linked to familial amyotrophic lateral sclerosis. J Biol Chem 283(20):13528–13537
15. Wang J, Slunt H, Gonzales V, Fromholt D, Coonfield M, Copeland NG, Jenkins NA, Borchelt DR (2003) Copper-binding-site-null SOD1 causes ALS in transgenic mice: aggregates of non-native SOD1 delineate a common feature. Hum Mol Genet 12(21):2753–2764
16. Schwarze SRHA, Vocero-Akbani A, Dowdy SF (1999) In vivo protein transduction: delivery of a biologically active protein into the mouse. Science 285(5433):1569–1572
17. Ye Y, Shibata Y, Yun C, Ron D, Rapoport TA (2004) A membrane protein complex mediates retro-translocation from the ER lumen into the cytosol. Nature 429(6994):841–847
18. Lilley BN, Ploegh HL (2004) A membrane protein required for dislocation of misfolded proteins from the ER. Nature 429(6994):834–840
19. Fujisawa T, Homma K, Yamaguchi N, Kadowaki H, Tsuburaya N, Naguro I, Matsuzawa A, Takeda K, Takahashi Y, Goto J et al (2012) A novel monoclonal antibody reveals a conformational alteration shared by amyotrophic lateral sclerosis-linked SOD1 mutants. Ann Neurol 72(5):739–749
20. Homma K, Fujisawa T, Tsuburaya N, Yamaguchi N, Kadowaki H, Takeda K, Nishitoh H, Matsuzawa A, Naguro I, Ichijo H (2013) SOD1 as a molecular switch for initiating the homeostatic ER stress response under zinc deficiency. Mol Cell 52(1):75–86
21. Chen X, Shang H, Qiu X, Fujiwara N, Cui L, Li XM, Gao TM, Kong J (2012) Oxidative modification of cysteine 111 promotes disulfide bond-independent aggregation of SOD1. Neurochem Res 37(4):835–845
22. Gaj T, Ojala DS, Ekman FK, Byrne LC, Limsirichai P, Schaffer DV (2017) In vivo genome editing improves motor function and extends survival in a mouse model of ALS. Sci Adv 3(12):eaar3952
23. Lim CKW, Gapinske M, Brooks AK, Woods WS, Powell JE, Zeballos CM, Winter J, Perez-Pinera P, Gaj T (2020) Treatment of a mouse model of ALS by in vivo base editing. Mol Ther 28(4):1177–1189
24. Foust KD, Salazar DL, Likhite S, Ferraiuolo L, Ditsworth D, Ilieva H, Meyer K, Schmelzer L, Braun L, Cleveland DW et al (2013) Therapeutic AAV9-mediated suppression of mutant SOD1 slows disease progression and extends survival in models of inherited ALS. Mol Ther 21(12):2148–2159
25. McCampbell A, Cole T, Wegener AJ, Tomassy GS, Setnicka A, Farley BJ, Schoch KM, Hoye ML, Shabsovich M, Sun L et al (2018) Antisense oligonucleotides extend survival and reverse decrement in muscle response in ALS models. J Clin Investig 128(8):3558–3567
26. Miller T, Cudkowicz M, Shaw PJ, Andersen PM, Atassi N, Bucelli RC, Genge A, Glass J, Ladha S, Ludolph AL et al (2020) Phase 1–2 trial of antisense oligonucleotide tofersen for SOD1 ALS. N Engl J Med 383(2):109–119
27. Mueller C, Berry JD, McKenna-Yasek DM, Gernoux G, Owegi MA, Pothier LM, Douthwright CL, Gelevski D, Luppino SD, Blackwood M et al (2020) SOD1 suppression with adeno-associated virus and microRNA in familial ALS. N Engl J Med 383(2):151–158
28. Ding H, Schwarz DS, Keene A, Affar EB, Fenton L, Xia X, Shi Y, Zamore PD, Xu Z (2003) Selective silencing by RNAi of a dominant allele that causes amyotrophic lateral sclerosis. Aging Cell 2(4):209–217
29. Raoul C, Abbas-Terki T, Bensadoun JC, Guillot S, Haase G, Szulc J, Henderson CE, Aebischer P (2005) Lentiviral-mediated silencing of SOD1 through RNA interference retards disease onset and progression in a mouse model of ALS. Nat Med 11(4):423–428
30. Bravo-Hernandez M, Tadokoro T, Navarro MR, Platoshyn O, Kobayashi Y, Marsala S, Miyanohara A, Juhas S, Juhasova J, Skalnikova H et al (2020) Spinal subpial delivery of AAV9 enables widespread gene silencing and blocks motoneuron degeneration in ALS. Nat Med 26(1):118–130
31. Powell JE, Lim CKW, Krishnan R, McCallister TX, Saporito-Magrina C, Zeballos MA, McPheron GD, Gaj T (2022) Targeted gene silencing in the nervous system with CRISPR–Cas13. Sci Adv 8(3):eabk2485
32. Ivannikov MV, Van Remmen H (2015) Sod1 gene ablation in adult mice leads to physiological changes at the neuromuscular junction similar to changes that occur in old wild-type mice. Free Radic Biol Med 84:254–262
33. Urushitani M, Ezzi SA, Julien JP (2007) Therapeutic effects of immunization with mutant superoxide dismutase in mice models of amyotrophic lateral sclerosis. Proc Natl Acad Sci USA 104(7):2495–2500
34. Rakhit R, Robertson J, Vande Velde C, Horne P, Ruth DM, Griffin J, Cleveland DW, Cashman NR, Chakrabartty A (2007) An

immunological epitope selective for pathological monomer-misfolded SOD1 in ALS. Nat Med 13(6):754–759
35. Liu HN, Tjostheim S, Dasilva K, Taylor D, Zhao B, Rakhit R, Brown M, Chakrabartty A, McLaurin J, Robertson J (2012) Targeting of monomer/misfolded SOD1 as a therapeutic strategy for amyotrophic lateral sclerosis. J Neurosci 32(26):8791–8799
36. Maier M, Welt T, Wirth F, Montrasio F, Preisig D, McAfoose J, Vieira FG, Kulic L, Spani C, Stehle T et al (2018) A human-derived antibody targets misfolded SOD1 and ameliorates motor symptoms in mouse models of amyotrophic lateral sclerosis. Sci Transl Med 10(470):eaah3924
37. Hill MD, Goyal M, Menon BK, Nogueira RG, McTaggart RA, Demchuk AM, Poppe AY, Buck BH, Field TS, Dowlatshahi D et al (2020) Efficacy and safety of nerinetide for the treatment of acute ischaemic stroke (ESCAPE-NA1): a multicentre, double-blind, randomised controlled trial. Lancet 395(10227):878–887
38. Chattopadhyay M, Valentine JS (2009) Aggregation of copper-zinc superoxide dismutase in familial and sporadic ALS. Antioxid Redox Signal 11(7):1603–1614
39. Chen X, Guan T, Li C, Shang H, Cui L, Li XM, Kong J (2012) SOD1 aggregation in astrocytes following ischemia/reperfusion injury: a role of NO-mediated S-nitrosylation of protein disulfide isomerase (PDI). J Neuroinflammation 9:237
40. Forman HJ, Fukuto JM, Torres M (2004) Redox signaling: thiol chemistry defines which reactive oxygen and nitrogen species can act as second messengers. Am J Physiol Cell Physiol 287(2):C246-256
41. Woo HA, Chae HZ, Hwang SC, Yang KS, Kang SW, Kim K, Rhee SG (2003) Reversing the inactivation of peroxiredoxins caused by cysteine sulfinic acid formation. Science 300(5619):653–656
42. Claiborne A, Yeh JI, Mallett TC, Luba J, Crane EJ 3rd, Charrier V, Parsonage D (1999) Protein-sulfenic acids: diverse roles for an unlikely player in enzyme catalysis and redox regulation. Biochemistry 38(47):15407–15416
43. Uchida K, Kawakishi S (1994) Identification of oxidized histidine generated at the active site of Cu, Zn-superoxide dismutase exposed to H_2O_2. Selective generation of 2-oxo-histidine at the histidine 118. J Biol Chem 269(4):2405–2410
44. Kurahashi T, Miyazaki A, Suwan S, Isobe M (2001) Extensive investigations on oxidized amino acid residues in H(2)O(2)-treated Cu, Zn-SOd protein with LC-ESI-Q-TOF-MS, MS/MS for the determination of the copper-binding site. J Am Chem Soc 123(38):9268–9278
45. Bruijn LI, Houseweart MK, Kato S, Anderson KL, Anderson SD, Ohama E, Reaume AG, Scott RW, Cleveland DW (1998) Aggregation and motor neuron toxicity of an ALS-linked SOD1 mutant independent from wild-type SOD1. Science 281(5384):1851–1854
46. Furukawa Y, Fu R, Deng HX, Siddique T, O'Halloran TV (2006) Disulfide cross-linked protein represents a significant fraction of ALS-associated Cu, Zn-superoxide dismutase aggregates in spinal cords of model mice. Proc Natl Acad Sci USA 103(18):7148–7153
47. Tiwari A, Hayward LJ (2003) Familial amyotrophic lateral sclerosis mutants of copper/zinc superoxide dismutase are susceptible to disulfide reduction. J Biol Chem 278(8):5984–5992
48. Tiwari A, Liba A, Sohn SH, Seetharaman SV, Bilsel O, Matthews CR, Hart PJ, Valentine JS, Hayward LJ (2009) Metal deficiency increases aberrant hydrophobicity of mutant superoxide dismutases that cause amyotrophic lateral sclerosis. J Biol Chem 284(40):27746–27758
49. Okado-Matsumoto A, Fridovich I (2002) Amyotrophic lateral sclerosis: a proposed mechanism. Proc Natl Acad Sci USA 99(13):9010–9014
50. Furukawa Y, O'Halloran TV (2006) Posttranslational modifications in Cu, Zn-superoxide dismutase and mutations associated with amyotrophic lateral sclerosis. Antioxid Redox Signal 8(5–6):847–867
51. Forsberg K, Andersen PM, Marklund SL, Brannstrom T (2011) Glial nuclear aggregates of superoxide dismutase-1 are regularly present in patients with amyotrophic lateral sclerosis. Acta Neuropathol 121(5):623–634
52. Kabashi E, Valdmanis PN, Dion P, Rouleau GA (2007) Oxidized/misfolded superoxide dismutase-1: the cause of all amyotrophic lateral sclerosis? Ann Neurol 62(6):553–559
53. Bunton-Stasyshyn RK, Saccon RA, Fratta P, Fisher EM (2015) SOD1 function and its implications for amyotrophic lateral sclerosis pathology: new and renascent themes. Neuroscientist 21(5):519–529